

# Gamma-ray Properties of Mixed Morphology Supernova Remnants

Jemma Pilosof

Supervisor: Dr Katie Auchettl

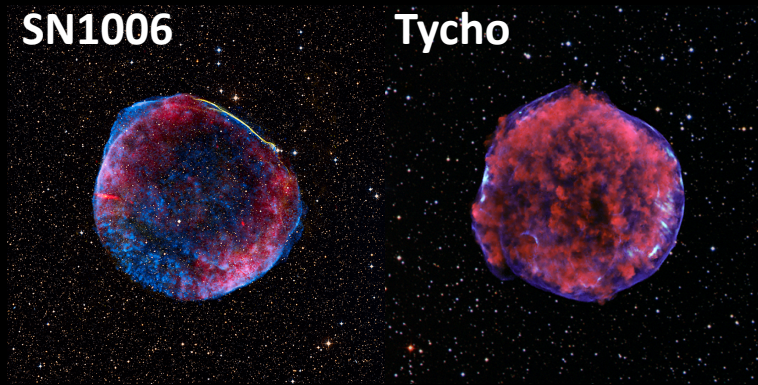
# Supernova Remnants (SNRs)

## Shell type:

- Bright radio/X-ray shell.
- Due to synchrotron radiation where particles have been accelerated at the shock front.

SN1006

Tycho

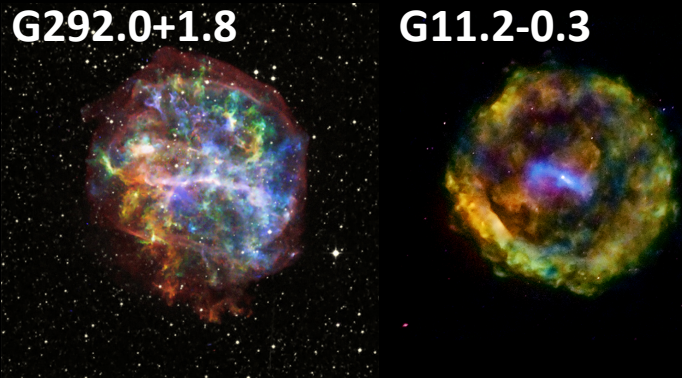


## Composite:

- Bright radio/X-ray shell - synchrotron radiation.
- Bright centre due to pulsar wind nebula (PWN) emitting non-thermal synchrotron radiation.

G292.0+1.8

G11.2-0.3

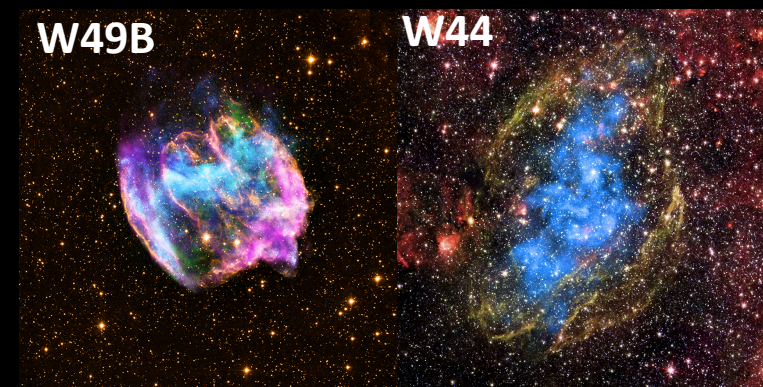


## Mixed Morphology (MM):

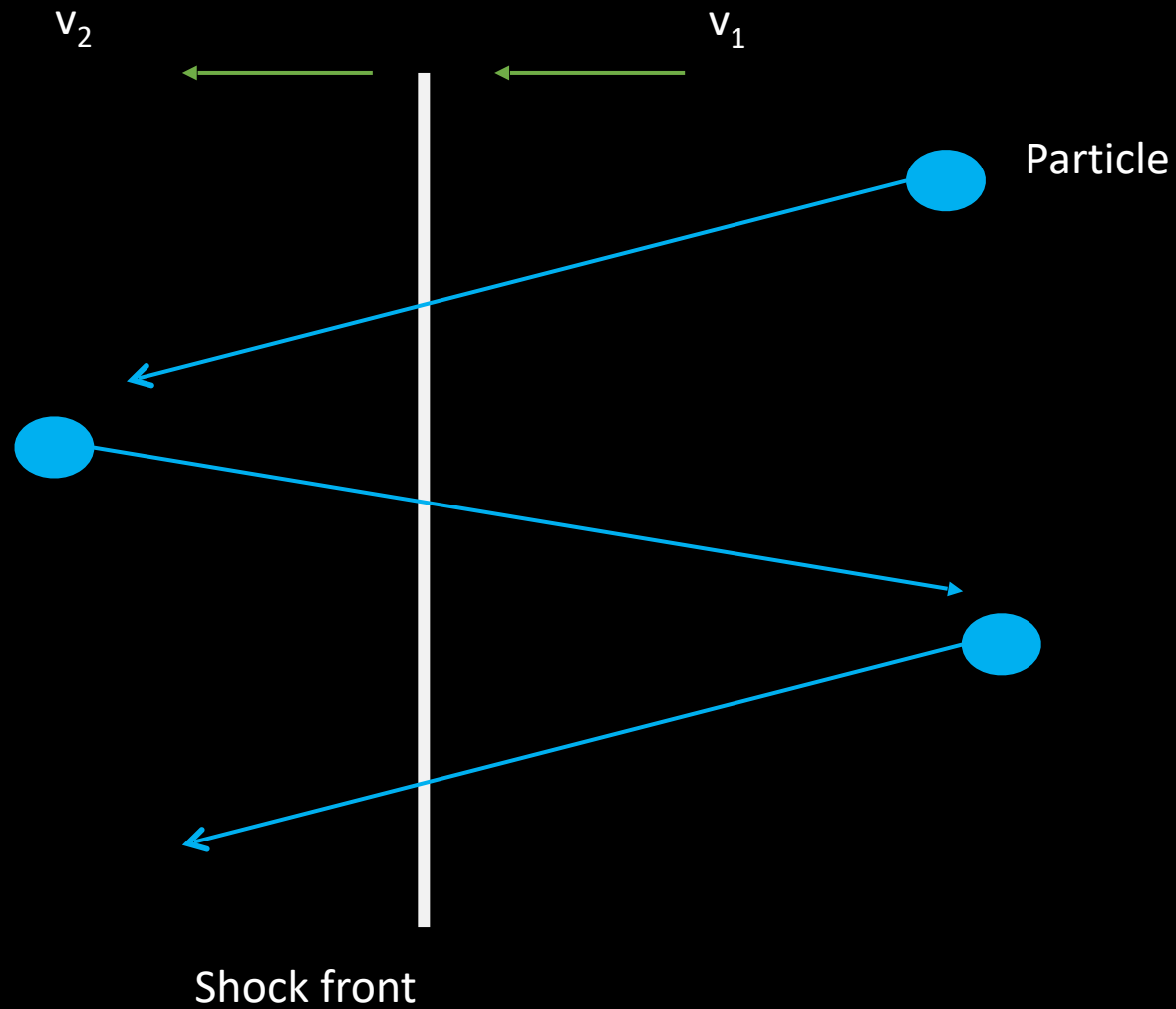
- Bright shell – synchrotron radiation.
- Bright centre due to thermal X-rays from swept up ISM.
- Most found to be interacting with molecular clouds.

W49B

W44



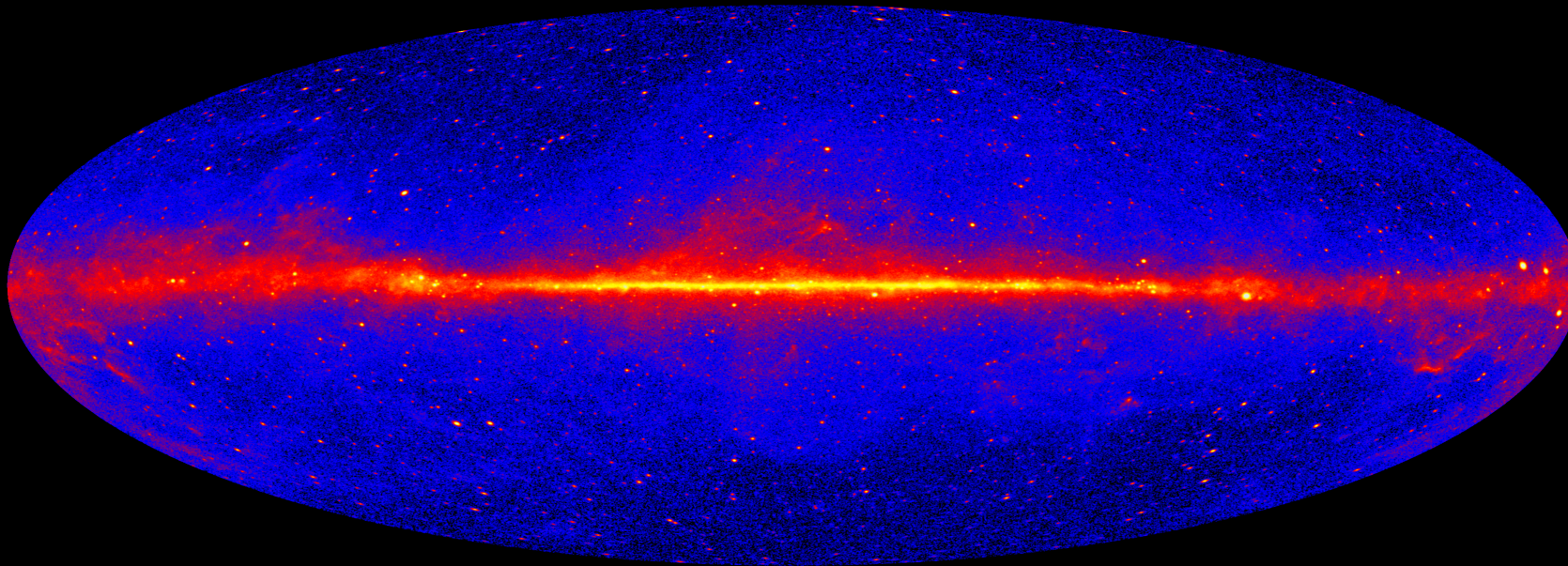
# Diffusive Shock acceleration



# Gamma-ray emission from MM SNRs

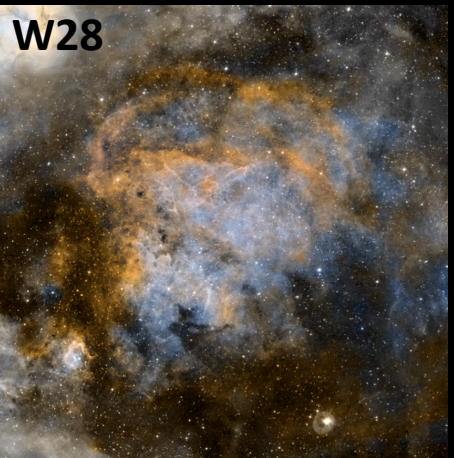
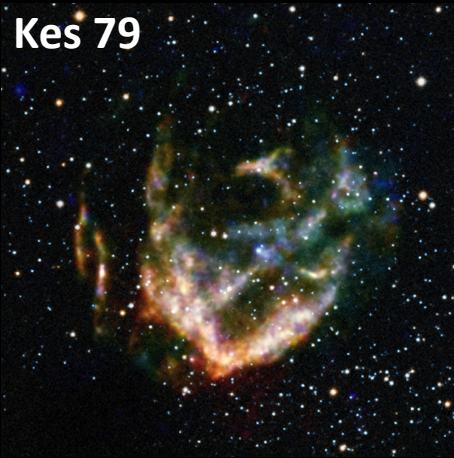
- Many are strong emitters of GeV gamma rays which is unexpected as most are middle aged.
- In an attempt to understand this many individual studies have been conducted but a consistent analysis of the population has not yet been undertaken.

**Aim:** Analyse 13.5 years of FERMI-LAT data for the population of MM SNRs in the Milky Way, to better understand the gamma ray and particle acceleration properties of this class.

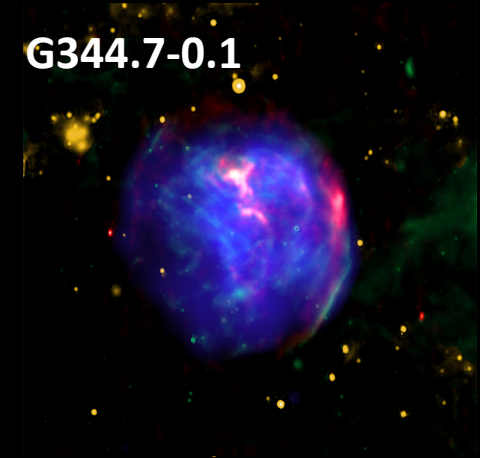


This view shows the entire sky at energies greater than 1 GeV based on 12 years of data from Fermi's Large Area Telescope. Credit: NASA/DOE/Fermi LAT Collaboration

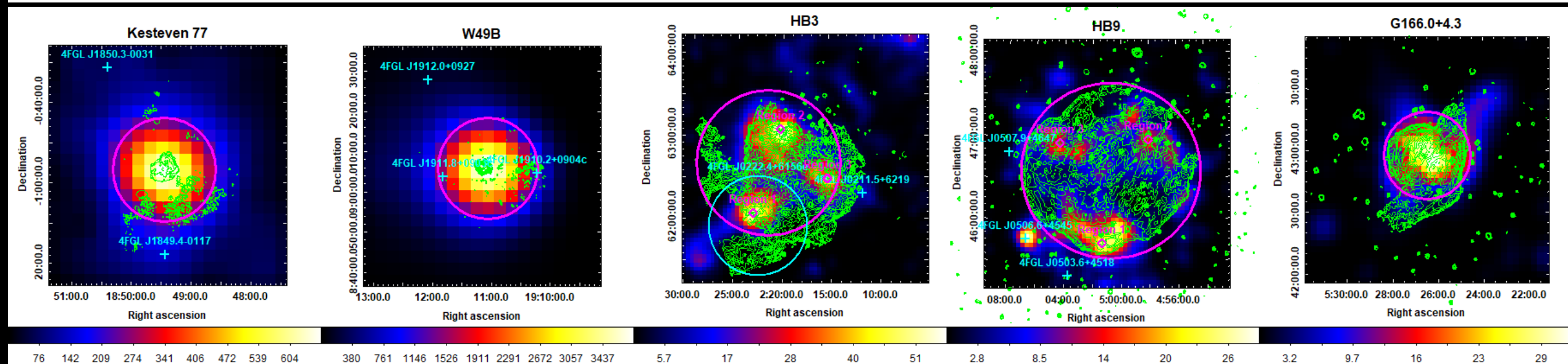
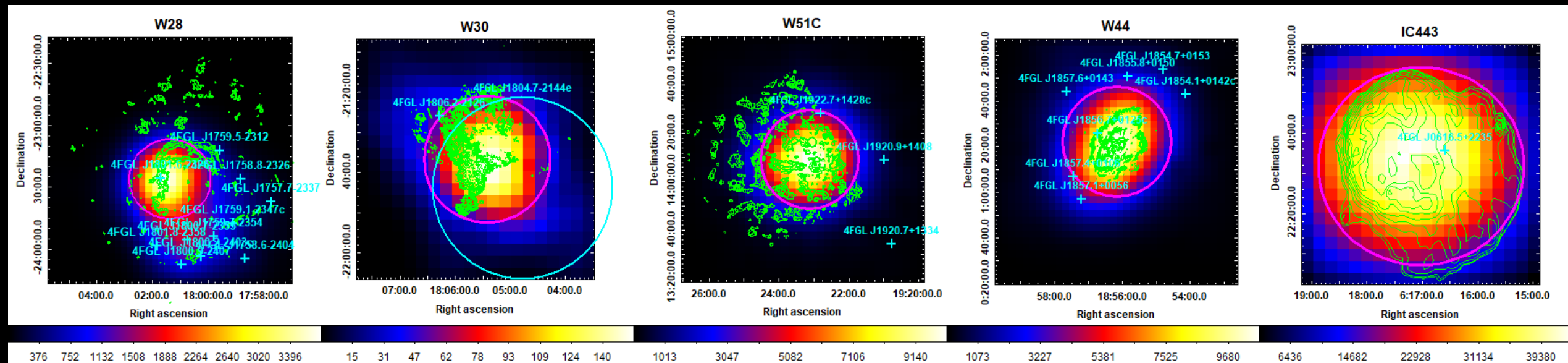
# Population



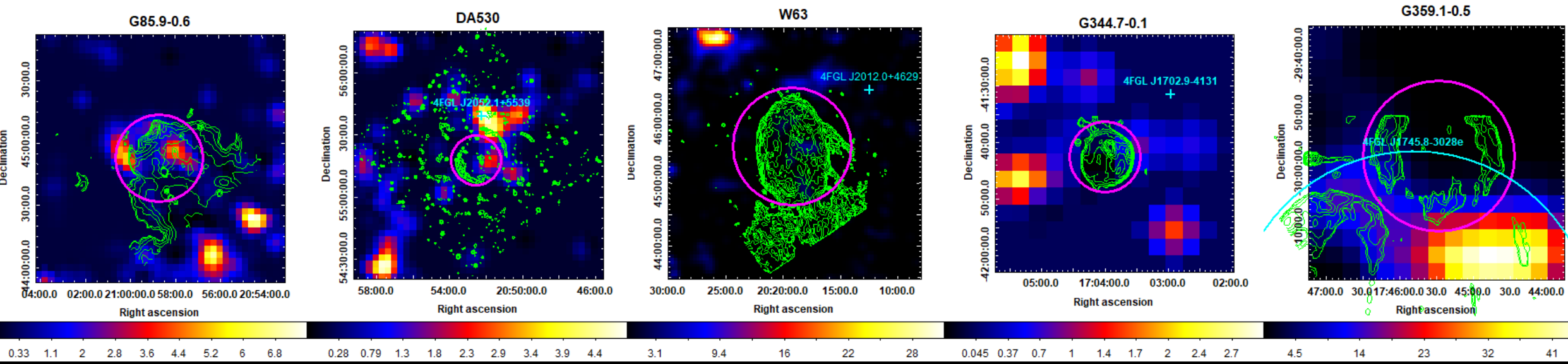
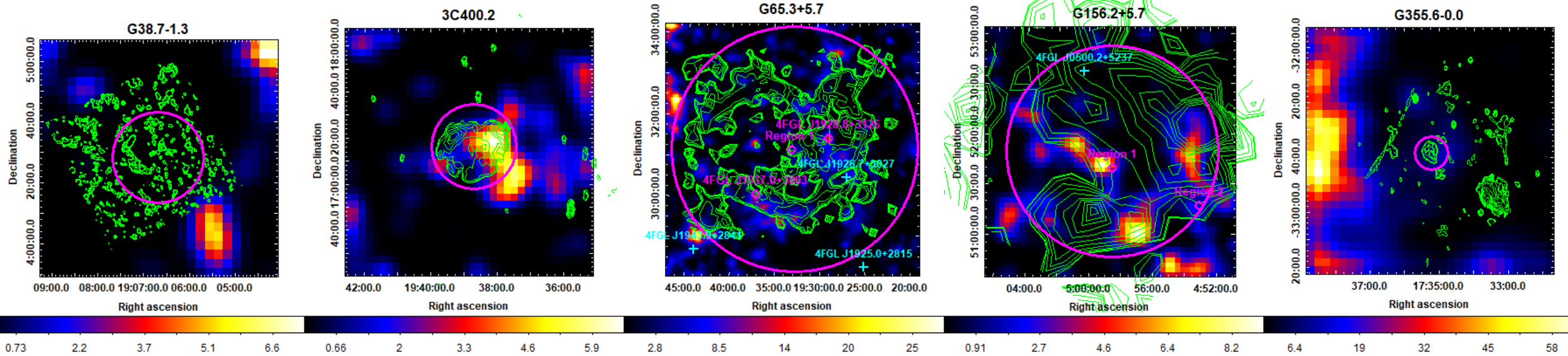
Remnant	Other names	Remnant	Other names
G0.0+0.0	Sgr A East	G116.9+0.2	CTB 1
G6.4-0.1	W28	G132.7+1.3	HB3
G8.7-0.1	W30	G156.2+5.7	
G21.8-0.6	Kes 69	G160.9+2.6	HB9
G31.9+0.0	Kes 77, 3C391	G166.0+4.3	VRO 42.05.01
G33.6+0.1	Kes 79, 4C00.7, HC13	G189.1+3.0	IC 443, HB21
G34.7-0.4	W44, 3C392	G272.2-3.2	
G38.7-1.3		G290.1-0.8	MSH 11-61A
G41.1-0.3	3C397	G298.6-0.0	
G43.3-0.2	W49B, 3C398	G304.6+0.1	Kes 17
G49.2-0.7	W51C	G311.5-0.3	
G53.6-2.2	3C400.2, NRAO 611	G327.4+0.4	Kes 27
G65.3+5.7		G337.8-0.1	Kes 41
G82.2+5.3	W63	G344.7-0.1	
G85.4+0.7		G346.6-0.2	
G85.9-0.6		G348.5+0.1	CTB 37A
G89.0+4.7	HB21	G352.7-0.1	
G93.3+6.9	DA 530, 4C(T)55.38.1	G355.6-0.0	
G93.7-0.2	CTB 104A, DA 551	G357.7-0.1	The Tornado, MSH 17-39
		G359.1-0.5	



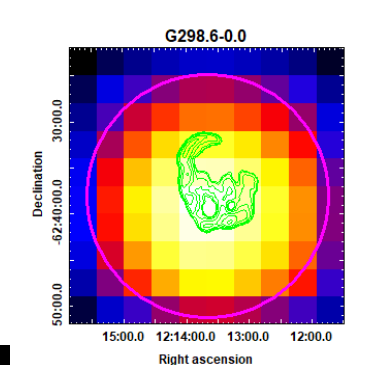
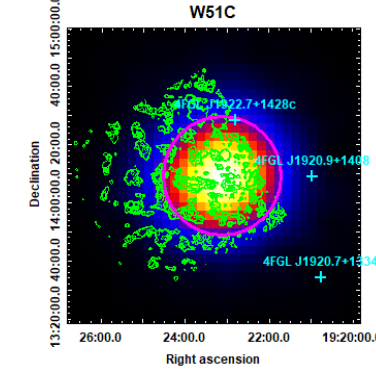
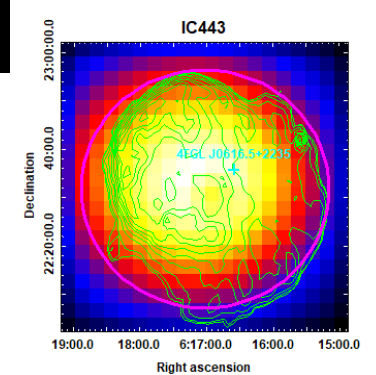
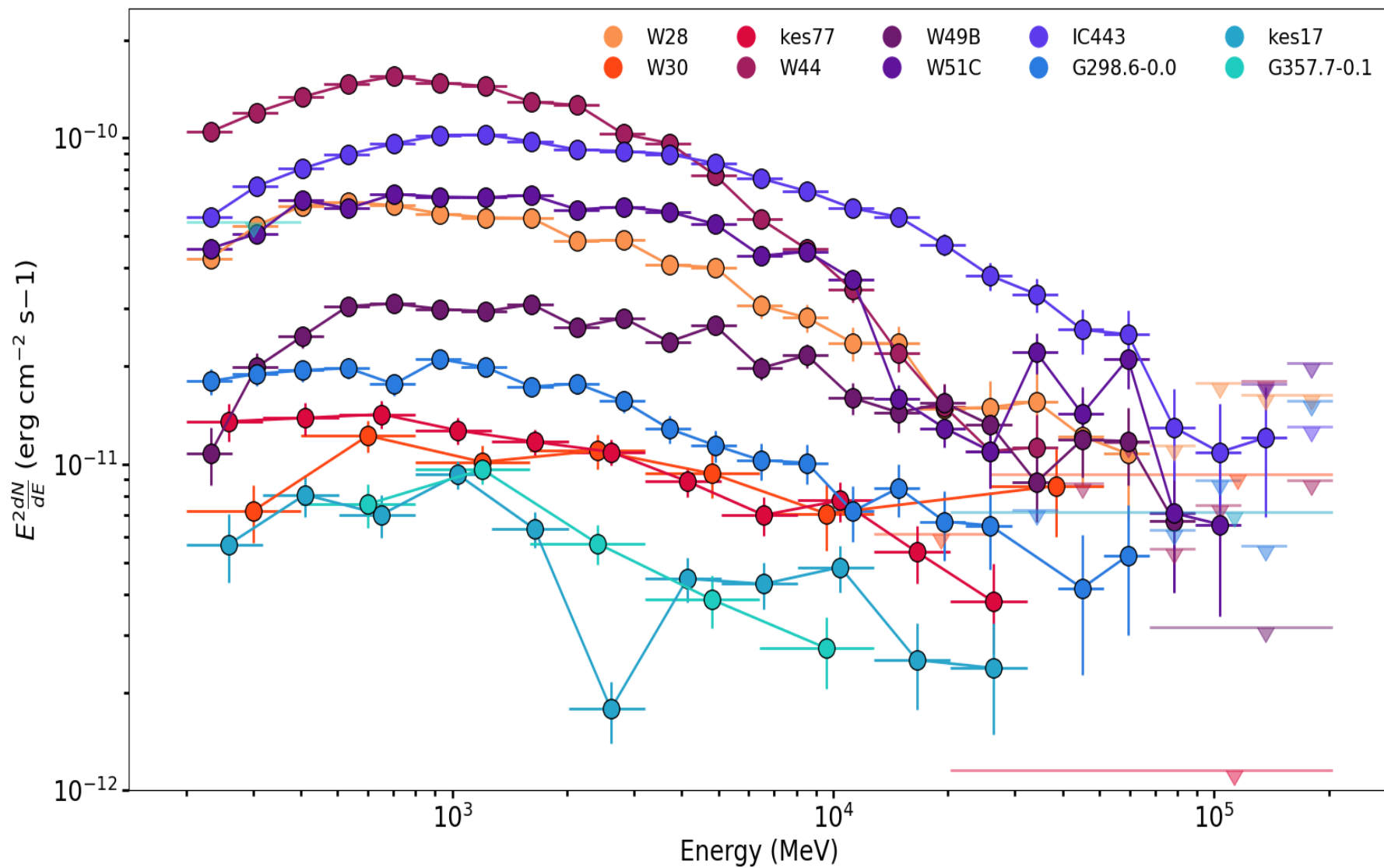
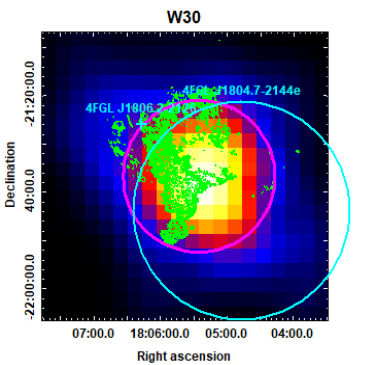
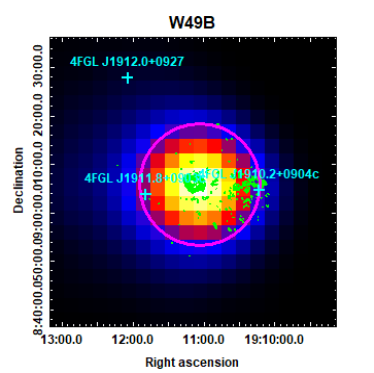
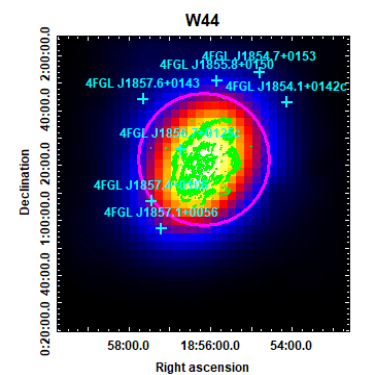
# Detection significance maps – Detected Sources



# Detection significance maps – Non-detected Sources



# Spectral Energy Distribution (SED)





# Fitting SEDs

Power law:

$$\frac{dN}{dE} = N_0 E^{-\Gamma}$$

Power law with Exponential Cut off:

$$\frac{dN}{dE} = N_0 E^{-\Gamma} e^{-\left(\frac{E}{E_c}\right)^{-\beta}}$$

Broken Power law:

$$\frac{dN}{dE} = N_0 E^{-\Gamma} \left( \left( 1 + \left( \frac{E}{E_b} \right) \right)^{\Gamma - \Gamma_2} \right)^{-1}$$

# Fitting SEDs

Power law:

$$\frac{dN}{dE} = N_0 E^{-\Gamma}$$

Power law with Exponential Cut off:

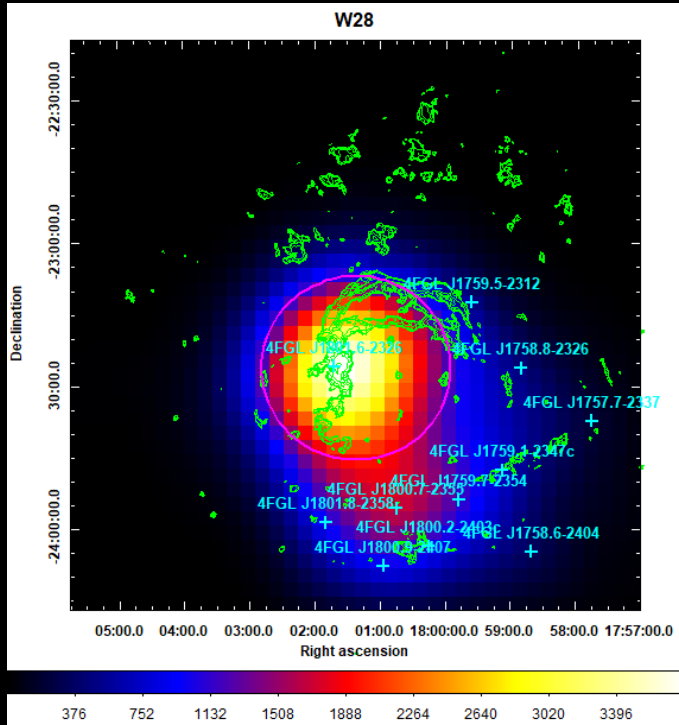
$$\frac{dN}{dE} = N_0 E^{-\Gamma} e^{-\left(\frac{E}{E_c}\right)^{-\beta}}$$

$\Gamma$  = Photon index

Broken Power law:

$$\frac{dN}{dE} = N_0 E^{-\Gamma} \left( \left( 1 + \left( \frac{E}{E_b} \right)^{\Gamma - \Gamma_2} \right)^{-1} \right)$$

# Fitting SEDs – W28



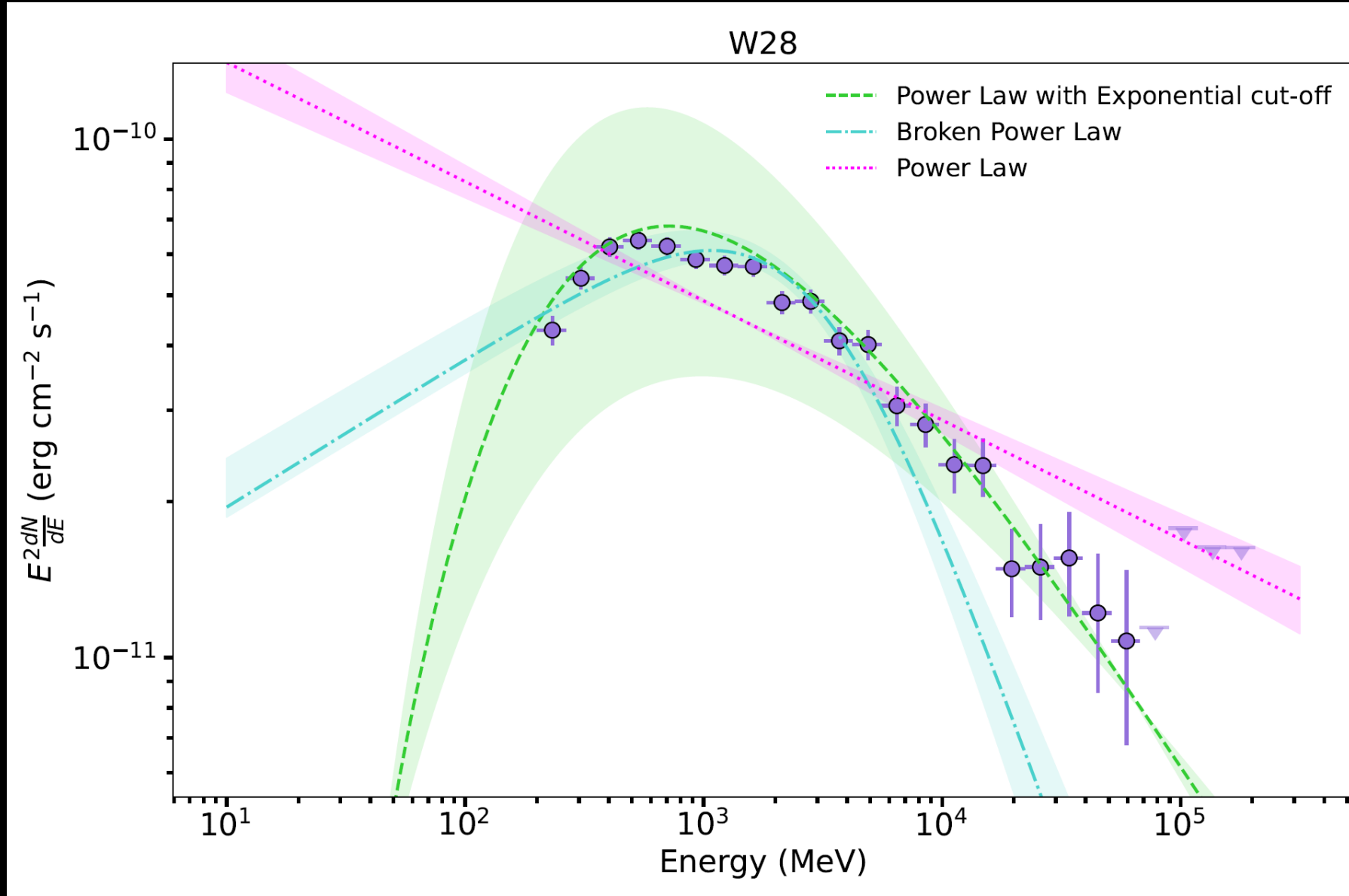
**Best Fit:**  
Power Law with Exponential Cut off

$$N_0 = 2_{-0.4}^{+0.5} \times 10^{-10} \text{ MeV}$$

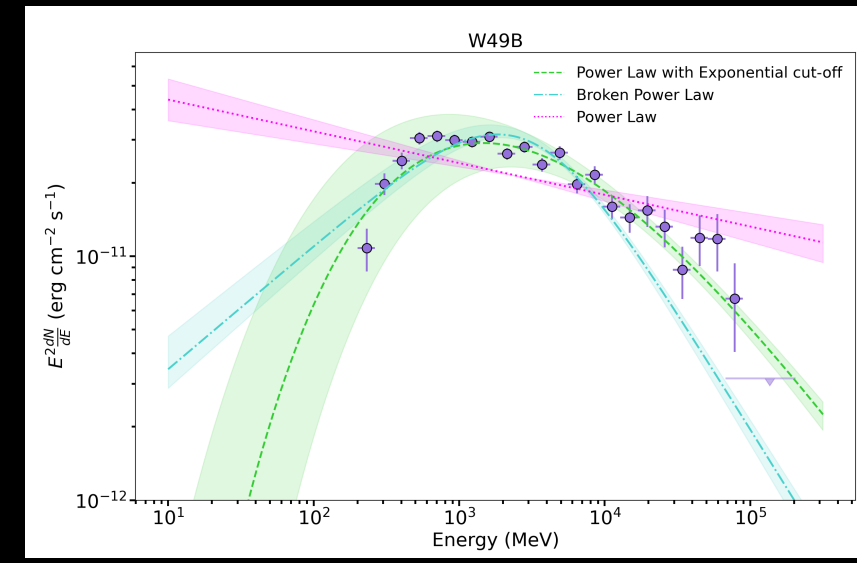
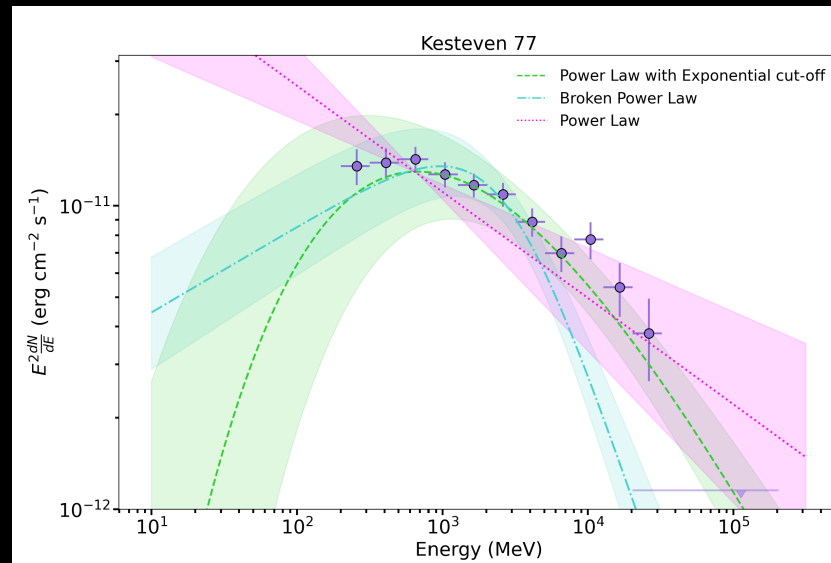
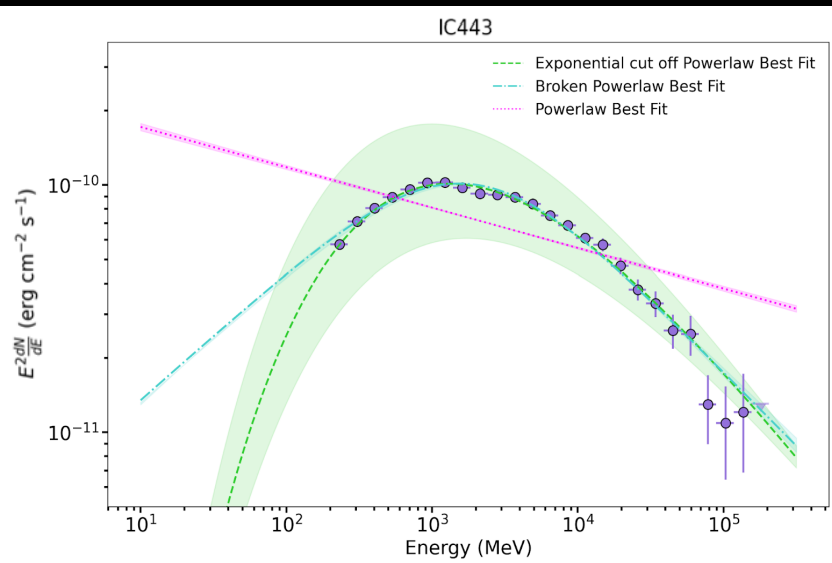
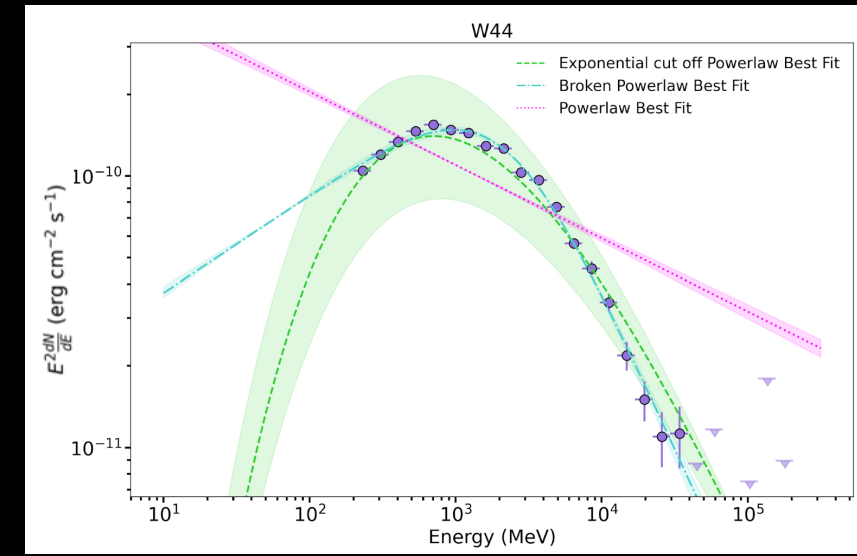
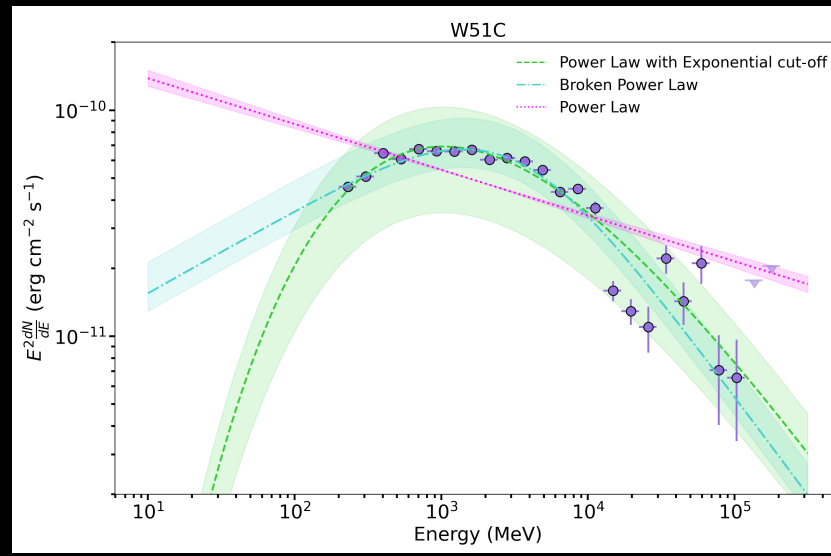
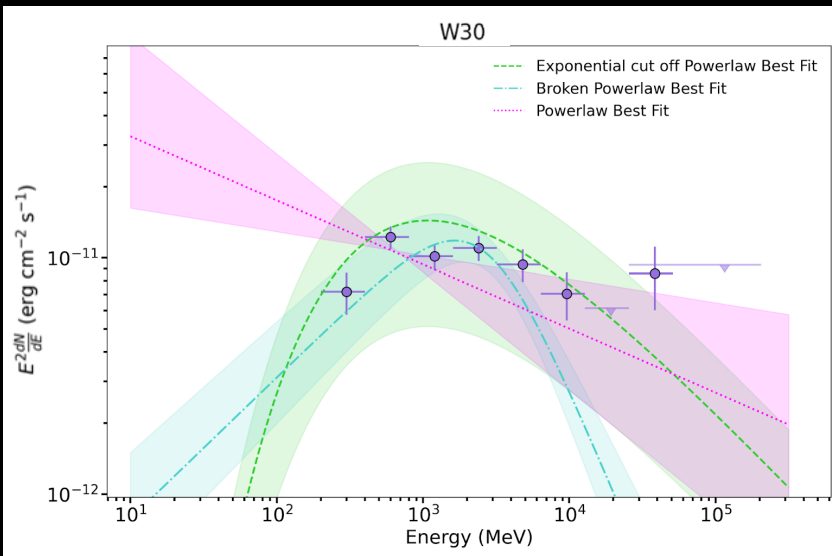
$$\Gamma = 2.7 \pm 0.1$$

$$E_C = 1.1_{-0.3}^{+0.9} \text{ GeV}$$

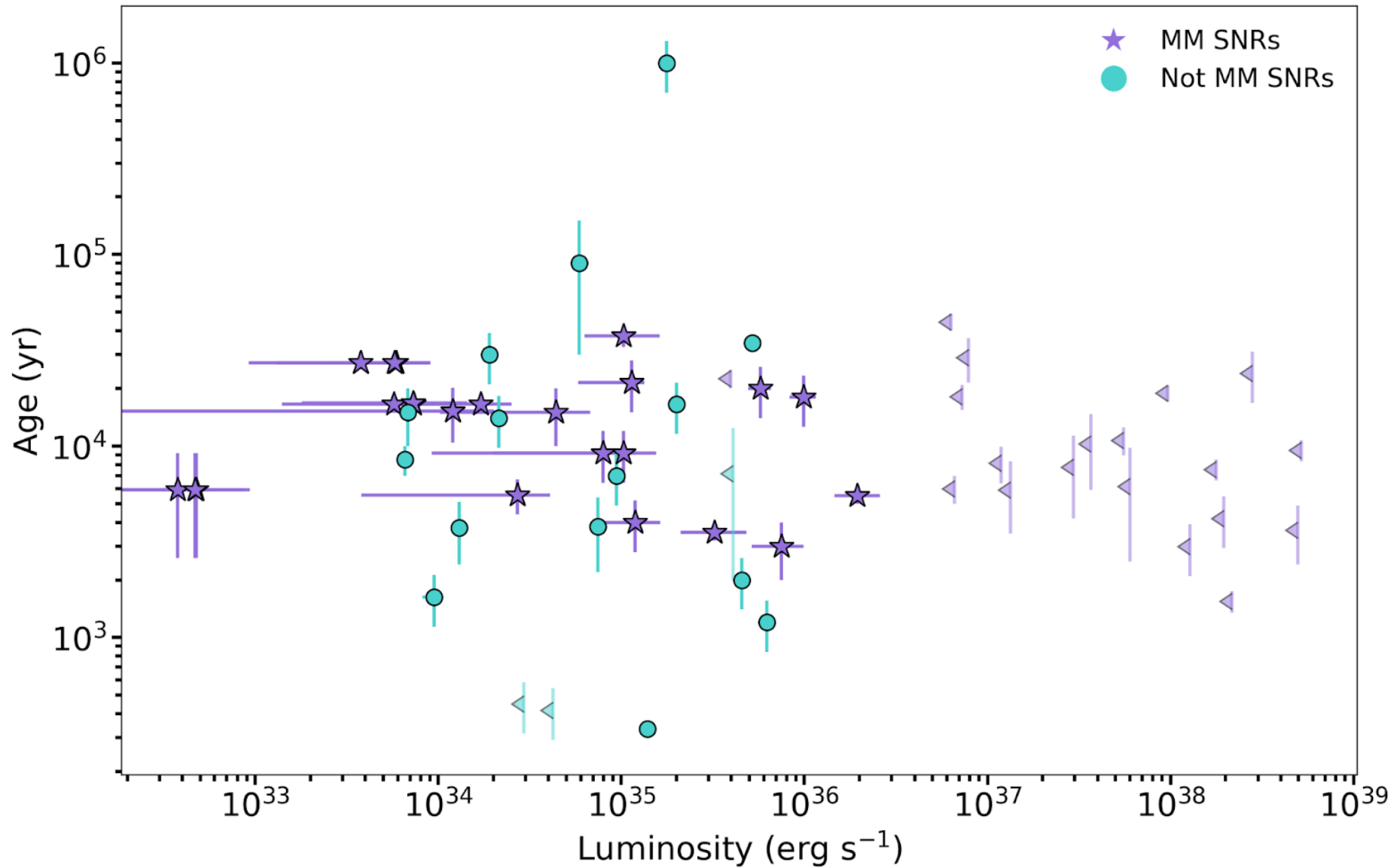
$$\beta = 0.6 \pm 0.1$$



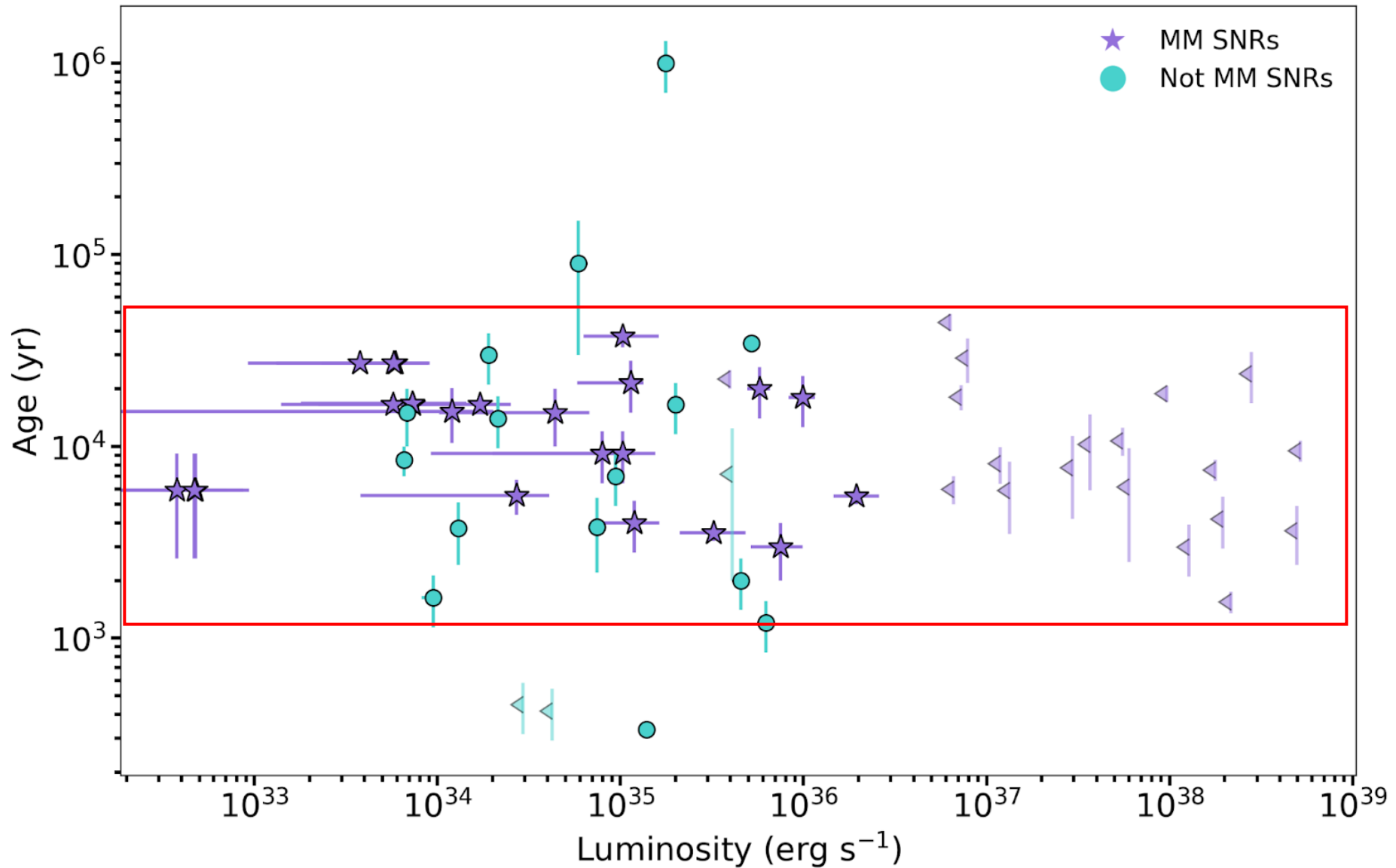
# Fitting SEDs



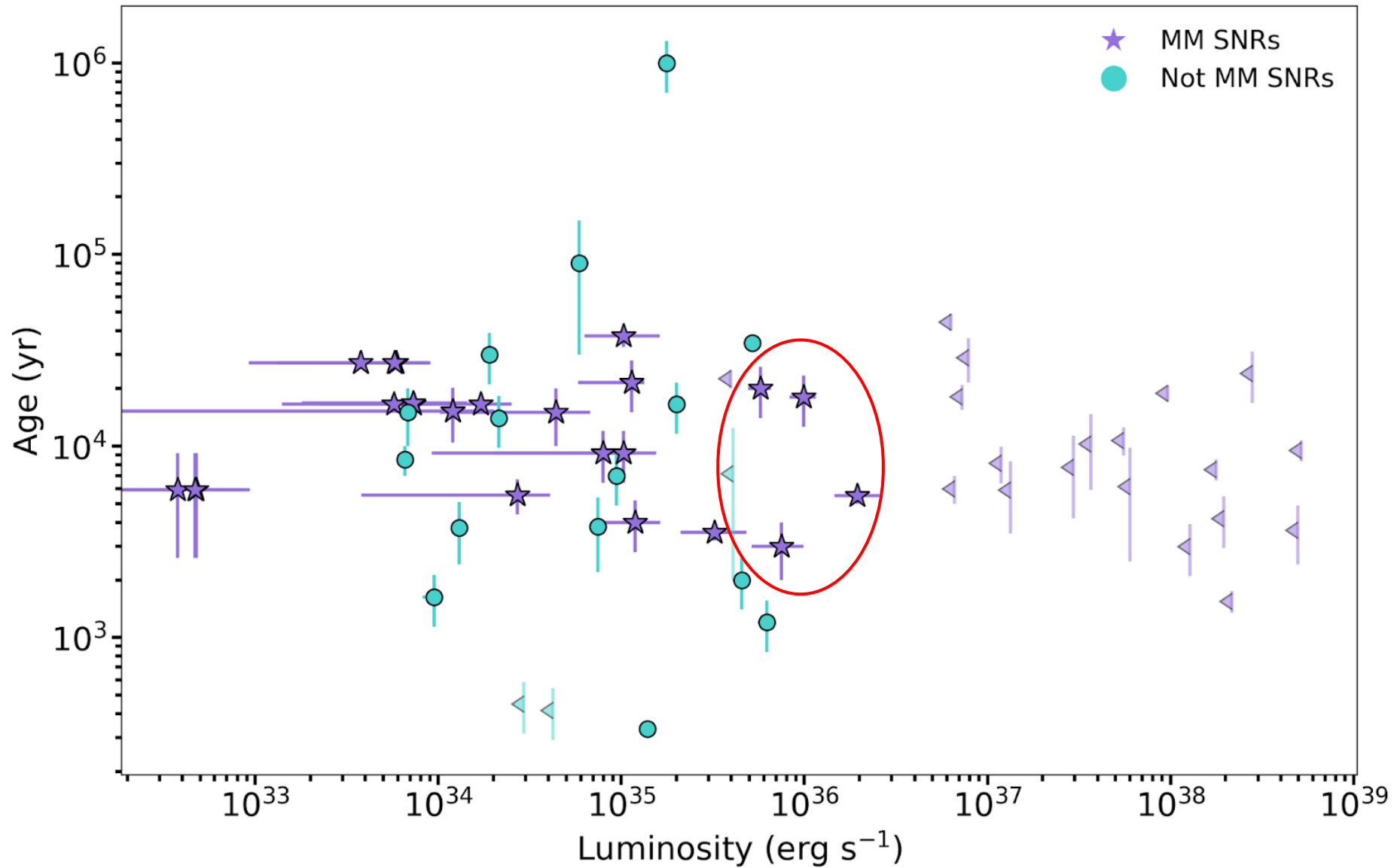
# Results - Age



# Results - Age



# Results - Age



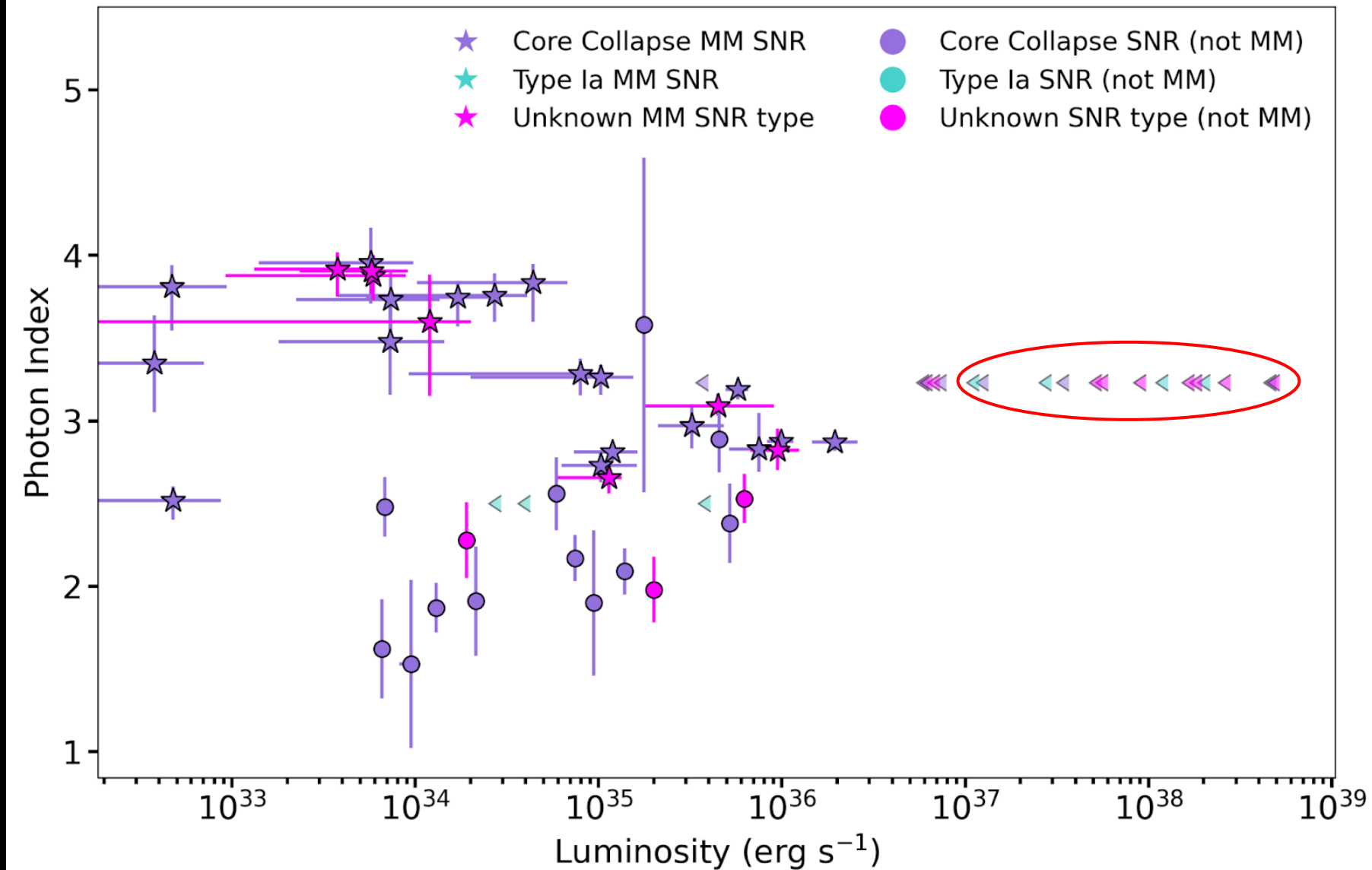




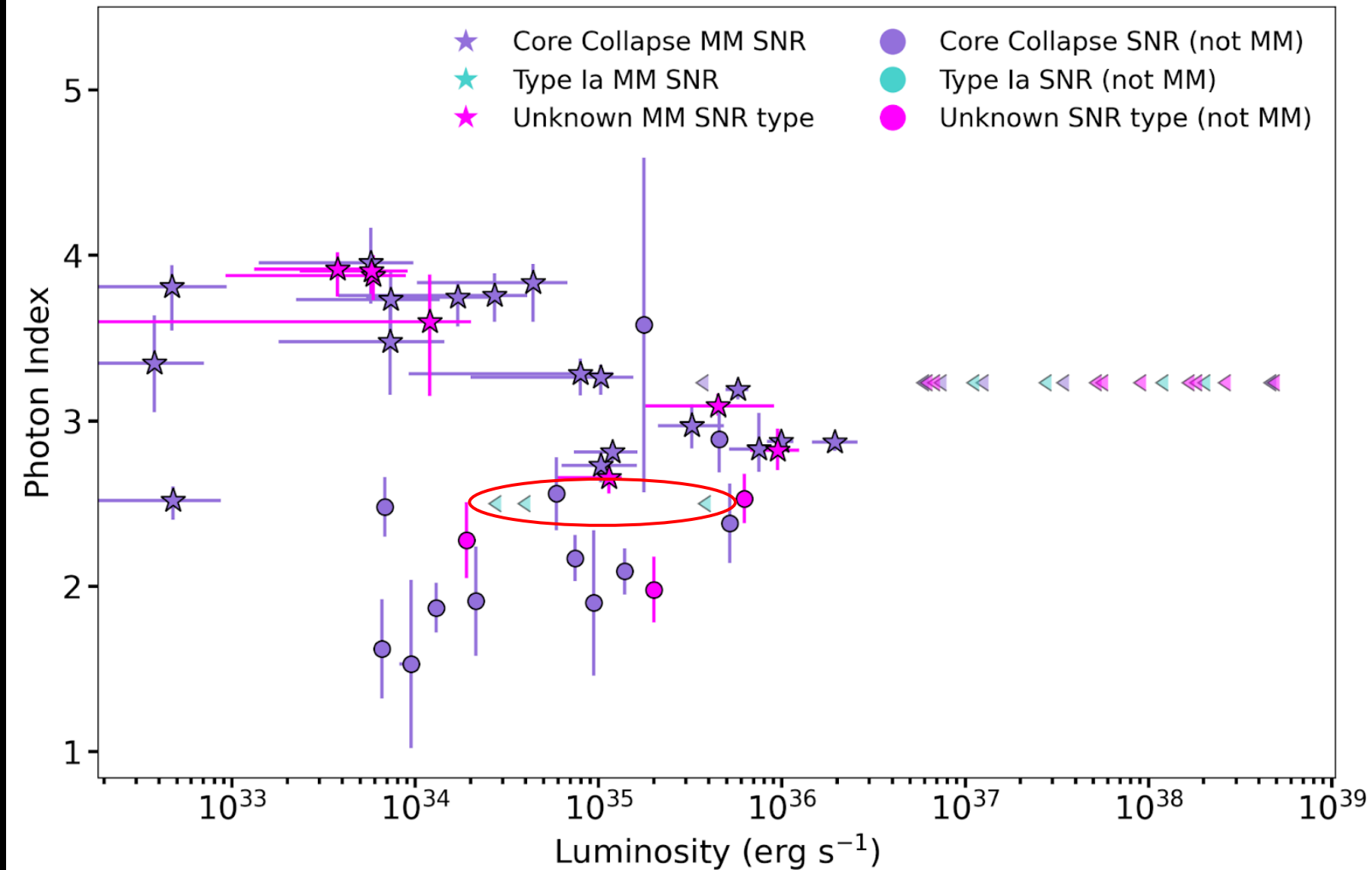




# Results - Type Ia vs Core-collapse



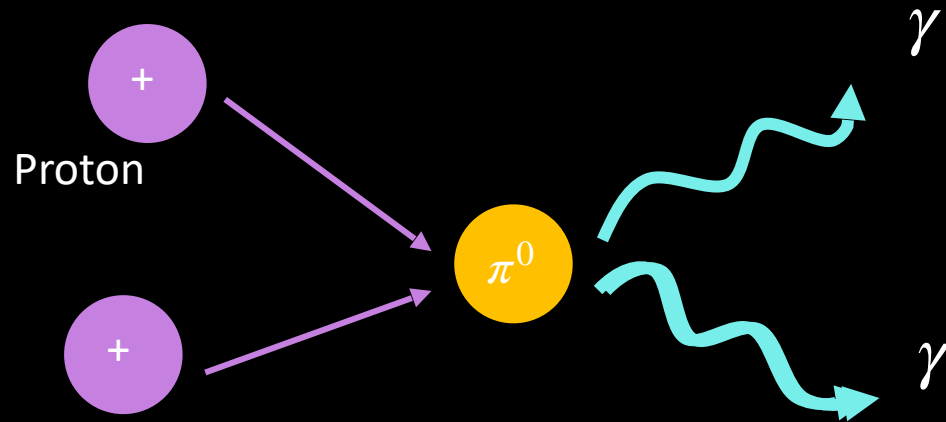
# Results - Type Ia vs Core-collapse



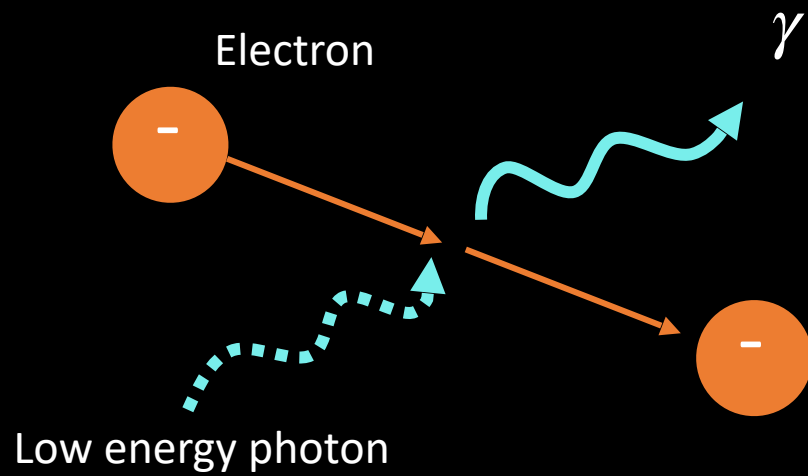


# Gamma-ray emission processes

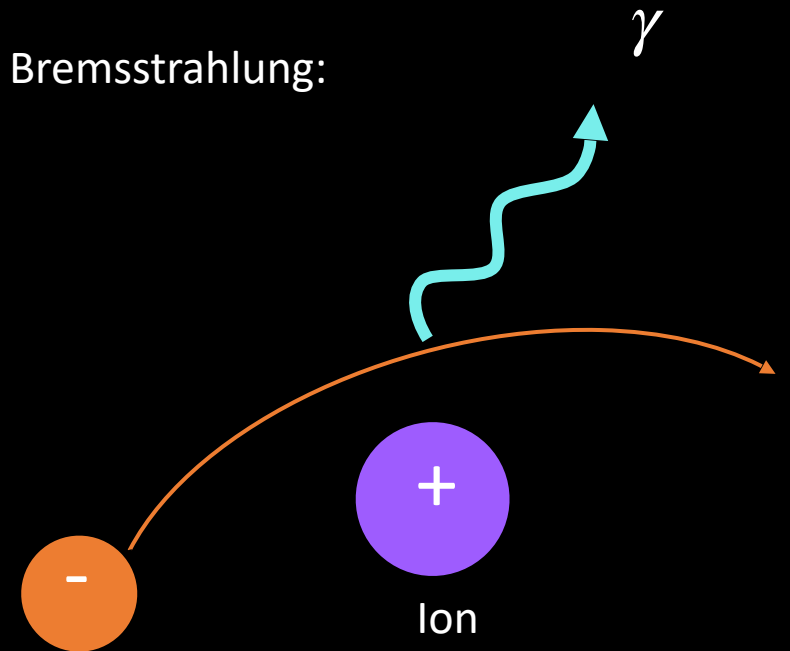
Neutral pion decay:



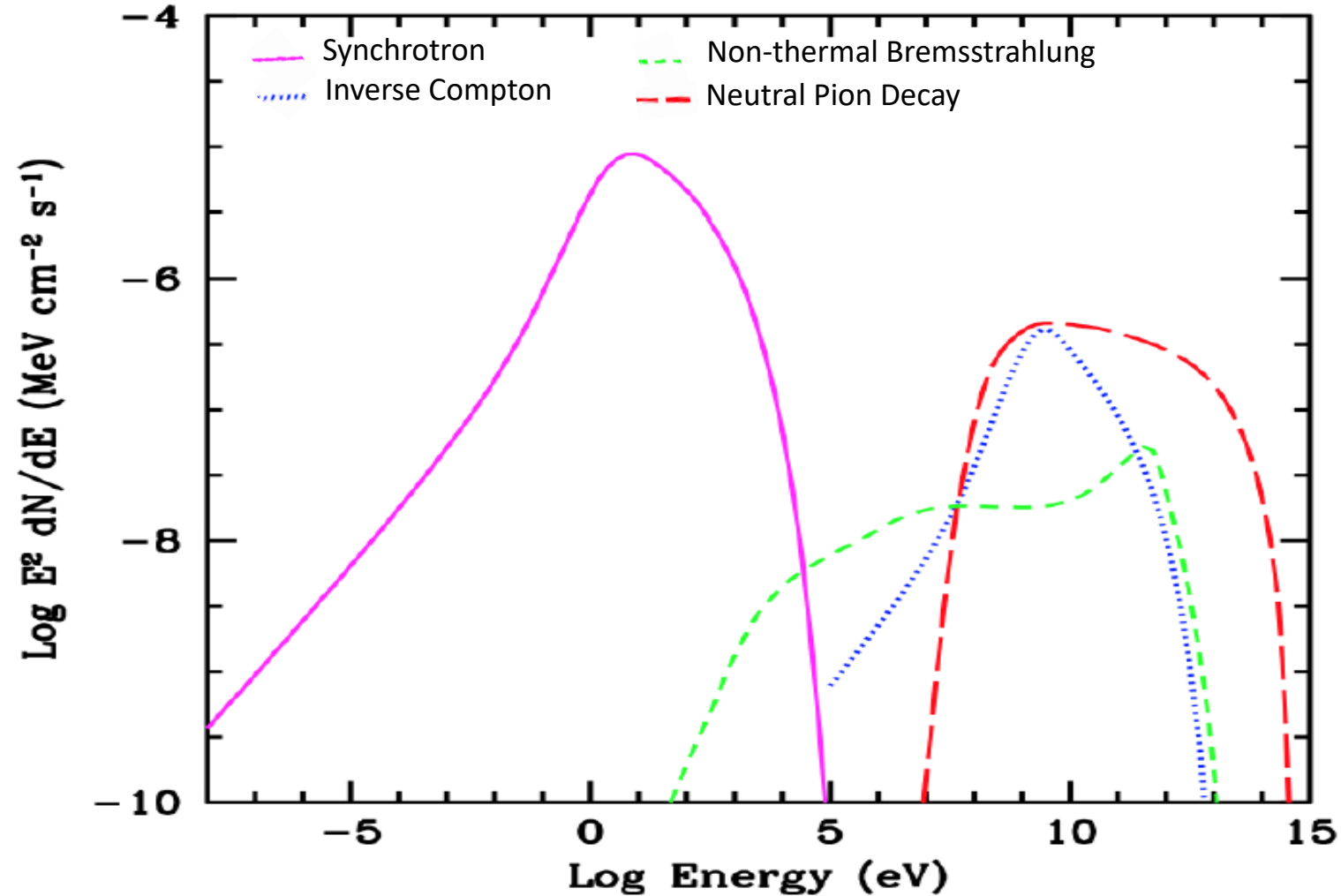
Inverse Compton Scattering:



Non-thermal Bremsstrahlung:

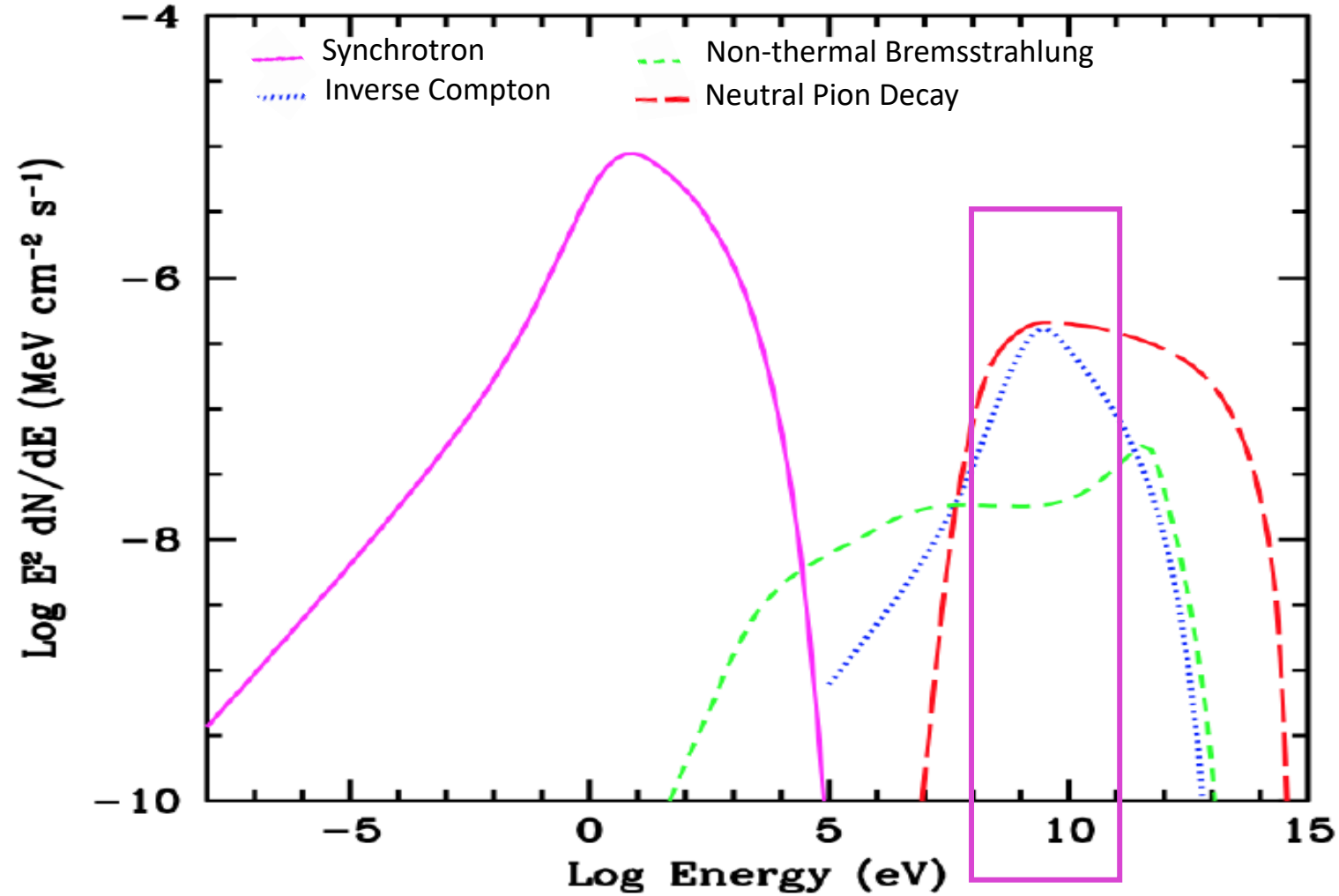


# Gamma-ray emission from SNRs



Simulated broadband spectrum from a supernova remnant undergoing efficient diffusive shock acceleration of electrons and protons (Slane et al 2015).

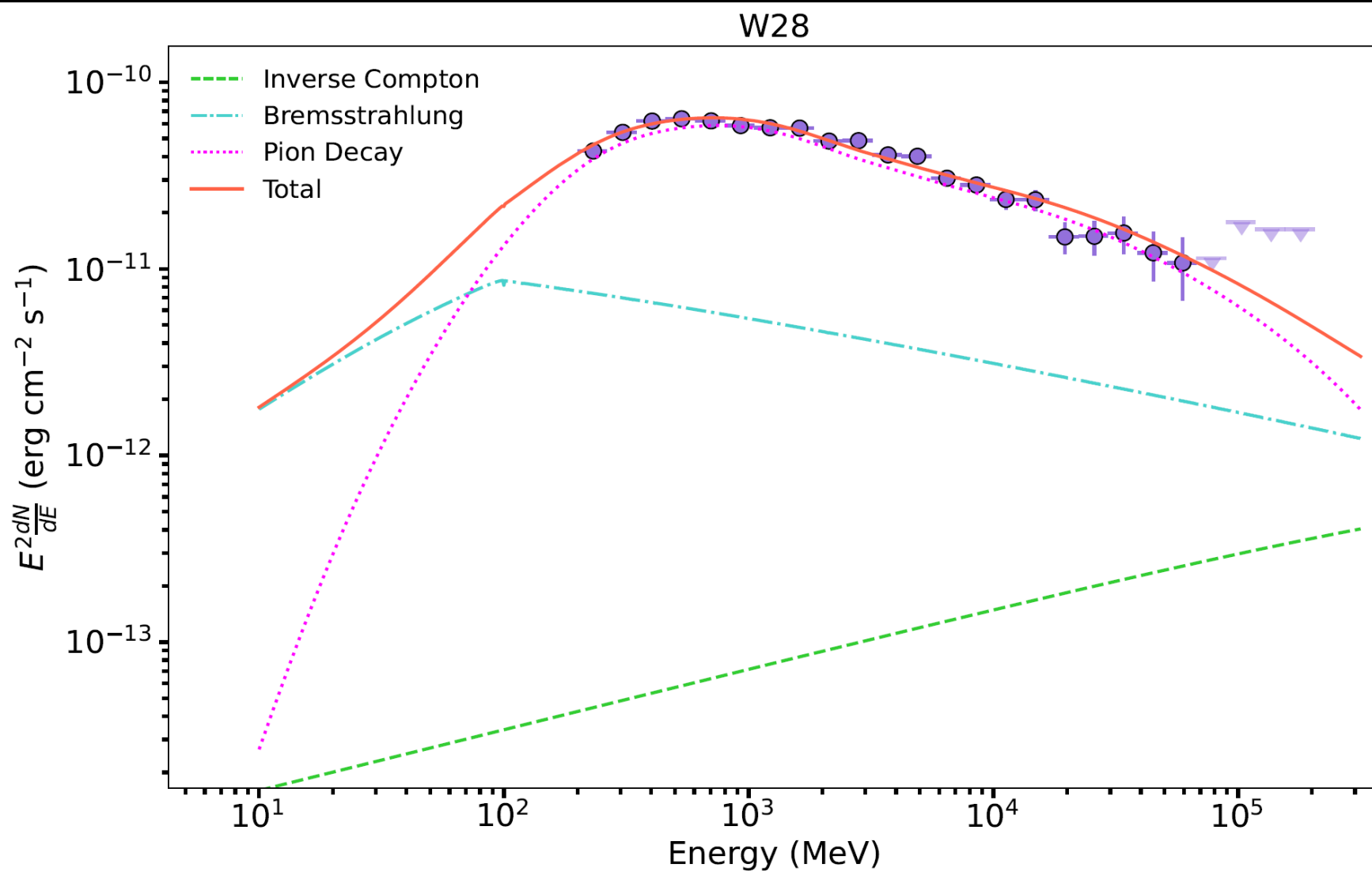
# Gamma-ray emission from SNRs



Simulated broadband spectrum from a supernova remnant undergoing efficient diffusive shock acceleration of electrons and protons (Slane et al 2015).



# Modelling the Origin of the Gamma-ray emission

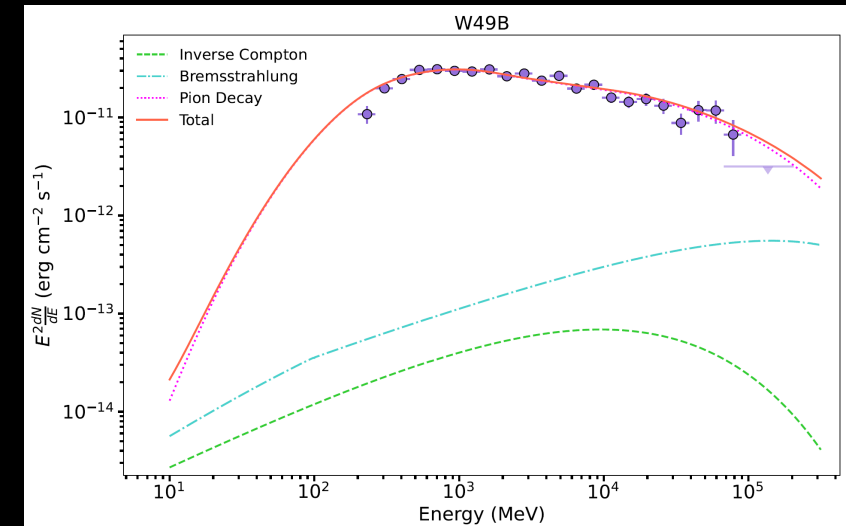
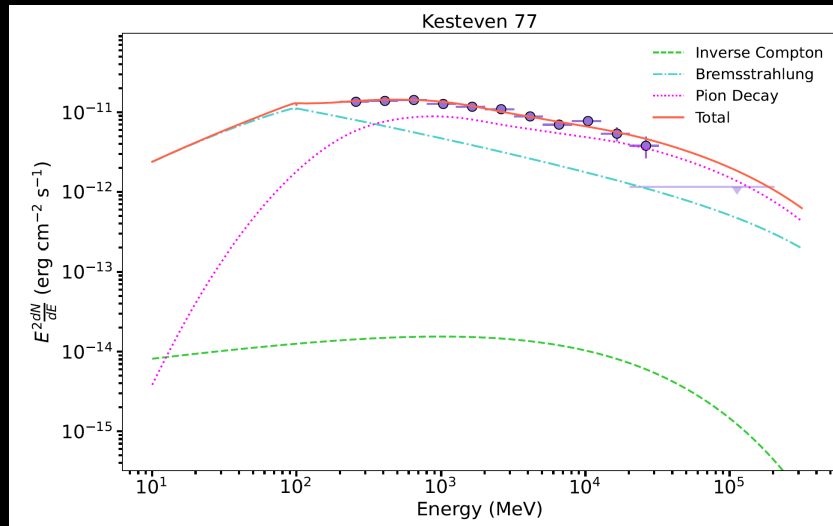
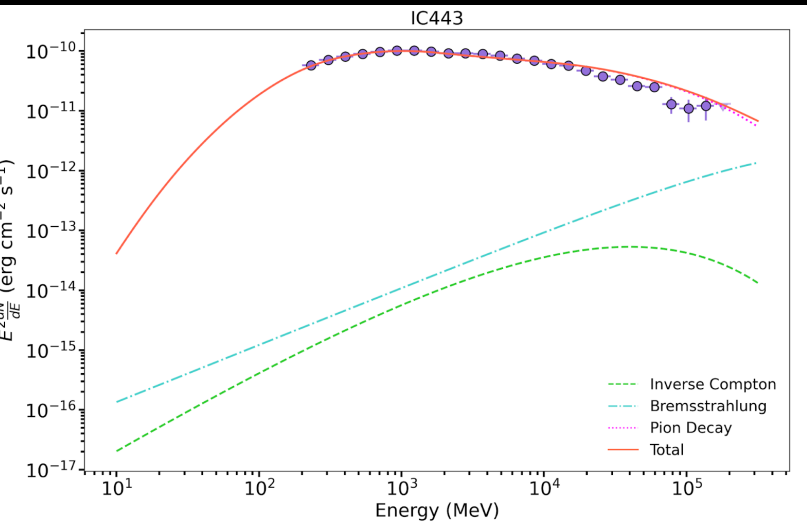
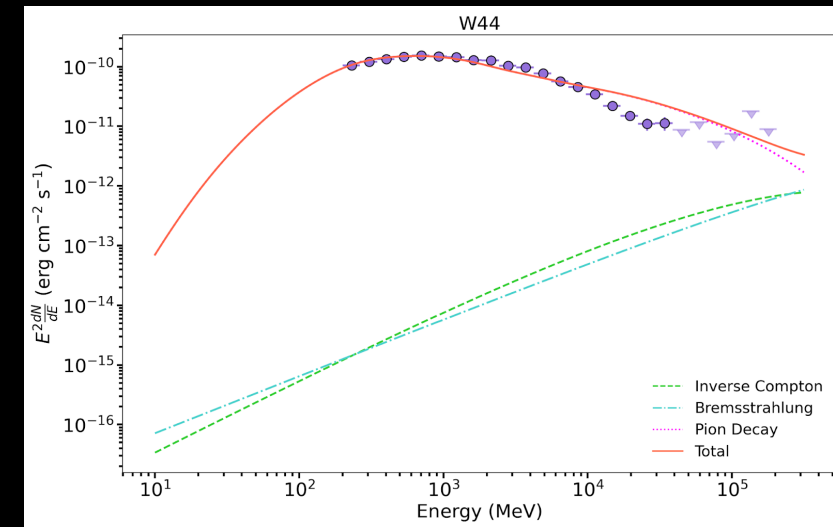
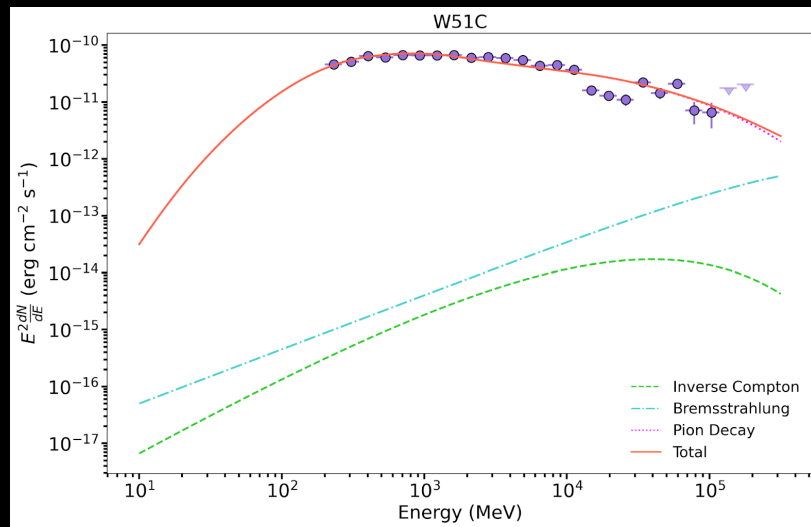
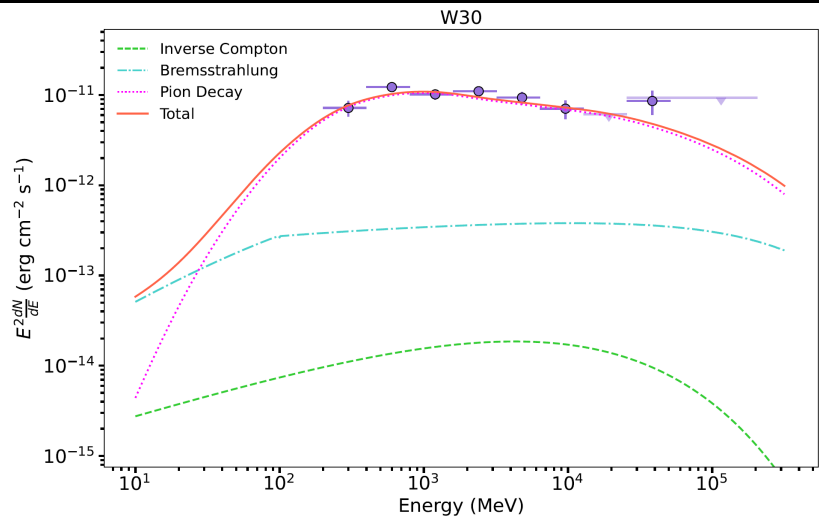


Density:  $62 \pm 6 \text{ cm}^{-3}$

Proton energy:  $1^{+0.3}_{-0.1} \times 10^{49} \text{ erg}$

Electron energy:  $3^{+3}_{-2} \times 10^{47} \text{ erg}$

# Origin of the Gamma-ray emission



# Density

Source	Amplitude $\times 10^{47} \text{ TeV}^{-1}$	$\Gamma_p$	$\Gamma_e$	$E_{cp}$ (TeV)	$E_{ce}$ (TeV)	$n_h$ ( $\text{cm}^{-3}$ )	$K_{ep}$ ( $\times 10^{-3}$ )	$\ln \mathcal{L}$
W28	$1.56^{+0.37}_{-0.37}$	$2.46^{+0.04}_{-0.04}$	$2.39^{+0.09}_{-0.19}$	$2.22^{+0.37}_{-0.28}$	$77.97^{+45.69}_{-30.29}$	$62.13^{+6.14}_{-6.07}$	$9.83^{+1.07}_{-1.28}$	-13.5
W44	$3.48^{+0.44}_{-0.45}$	$2.57^{+0.01}_{-0.01}$	$0.54^{+0.06}_{-0.04}$	$1.06^{+0.01}_{-0.01}$	$4.56^{+1.31}_{-1.33}$	$131.74^{+15.49}_{-12.69}$	$5.02^{+0.61}_{-0.6}$	-205.31
IC443	$0.71^{+0.08}_{-0.06}$	$2.22^{+0.01}_{-0.01}$	$0.12^{+0.02}_{-0.02}$	$0.99^{+0.0005}_{-0.0004}$	$0.97^{+0.003}_{-0.005}$	$519.26^{+31.70}_{-30.47}$	$10.92^{+1.05}_{-1.23}$	-46.99
W51C	$3.01^{+0.59}_{-0.54}$	$2.36^{+0.02}_{-0.01}$	$0.11^{+0.02}_{-0.03}$	$0.99^{+0.002}_{-0.002}$	$0.97^{+0.006}_{-0.007}$	$599.64^{+104.32}_{-96.79}$	$10.64^{+2.95}_{-2.43}$	-163.48
W49B	$97.3^{+29.3}_{-19.6}$	$2.27^{+0.03}_{-0.03}$	$1.91^{+0.27}_{-0.5}$	$1.47^{+0.15}_{-0.16}$	$0.98^{+0.009}_{-0.009}$	$50.59^{+11.72}_{-13.04}$	$10.42^{+1.94}_{-1.7}$	-21.78
G298.6-0.0	$23.7^{+10.50}_{-6.91}$	$2.44^{+0.04}_{-0.05}$	$2.05^{+0.35}_{-0.49}$	$1.44^{+0.24}_{-0.25}$	$0.98^{+0.010}_{-0.009}$	$50.94^{+14.16}_{-12.70}$	$10.44^{+3.03}_{-3.58}$	-7.11
Kesteven 77	$9.31^{+5.08}_{-3.46}$	$2.33^{+0.14}_{-0.17}$	$2.52^{+0.06}_{-0.12}$	$1.3^{+0.12}_{-0.16}$	$0.98^{+0.005}_{-0.005}$	$53.62^{+16.08}_{-10.65}$	$10.69^{+3.47}_{-3.00}$	-3.96
W30	$5.21^{+6.94}_{-2.51}$	$2.25^{+0.10}_{-0.15}$	$2.02^{+0.29}_{-0.62}$	$1.47^{+0.45}_{-0.35}$	$0.98^{+0.01}_{-0.01}$	$48.12^{+33.83}_{-24.57}$	$10.05^{+6.99}_{-5.40}$	-3.09
Kesteven 17	$19.8^{+19.20}_{-19.80}$	$2.39^{+0.13}_{-0.62}$	$2.06^{+0.52}_{-0.93}$	$1.45^{+0.22}_{-0.20}$	$0.98^{+0.009}_{-0.007}$	$48.12^{+22.12}_{-15.34}$	$9.91^{+5.17}_{-4.07}$	-3.84
G357.7-0.1	$6.85^{+10.50}_{-6.85}$	$2.5^{+0.24}_{-0.31}$	$2.02^{+0.61}_{-0.96}$	$1.42^{+0.24}_{-0.19}$	$0.97^{+0.01}_{-0.01}$	$50.03^{+20.84}_{-23.43}$	$9.95^{+4.61}_{-5.27}$	-4.38

- Density ranges between 48-600  $\text{cm}^{-3}$ .
- X-ray densities range between 0.01-10  $\text{cm}^{-3}$ .
- This discrepancy may be due to the presence of cold clumps of material that do not emit in thermal X-rays.

# Particle Energy

Source	$W_p$ $\times 10^{49}$ ergs	$W_{eBrem}$ $\times 10^{47}$ ergs	$W_{eIC}$ $\times 10^{46}$ ergs	$W_e$ $\times 10^{47}$ ergs	$W_{ep}$ $\times 10^{49}$ ergs
W28	$1.16^{+0.16}_{-0.33}$	$1.8^{+2.68}_{-1.28}$	$7.63^{+7.64}_{-4.17}$	$2.56^{+3.44}_{-1.69}$	$1.18^{+0.19}_{-0.34}$
W44	$4.2^{+0.50}_{-0.54}$	$0.21^{+0.01}_{-0.008}$	$2.14^{+0.95}_{-0.81}$	$0.43^{+0.19}_{-0.16}$	$4.2^{+0.50}_{-0.54}$
IC443	$0.17^{+0.01}_{-0.01}$	$0.011^{+0.002}_{-0.002}$	$0.11^{+0.02}_{-0.02}$	$0.023^{+0.004}_{-0.005}$	$0.17^{+0.01}_{-0.01}$
W51C	$1.33^{+0.26}_{-0.18}$	$0.05^{+0.03}_{-0.01}$	$0.47^{+0.14}_{-0.14}$	$0.09^{+0.03}_{-0.03}$	$1.33^{+0.26}_{-0.18}$
W49B	$29.37^{+9.97}_{-5.53}$	$9.22^{+25.8}_{-6.40}$	$73.35^{+121.96}_{-45.98}$	$16.56^{+38.00}_{-11.00}$	$29.54^{+10.35}_{-5.64}$
G298.6-0.0	$15.7^{+5.16}_{-3.52}$	$4.55^{+32.16}_{-3.74}$	$30.58^{+108.25}_{-23.39}$	$7.61^{+32.99}_{-6.08}$	$15.78^{+5.59}_{-3.58}$
Kesteven 77	$3.48^{+1.47}_{-1.25}$	$34.25^{+32.05}_{-23.55}$	$99.59^{+84.24}_{-60.91}$	$44.21^{+40.47}_{-29.64}$	$3.92^{+1.88}_{-1.55}$
W30	$1.35^{+1.33}_{-0.56}$	$0.82^{+4.38}_{-0.73}$	$5.62^{+18.80}_{-4.80}$	$1.38^{+36.25}_{-1.21}$	$1.36^{+1.39}_{-0.58}$
Kesteven 17	$10.68^{+6.54}_{-10.68}$	$3.18^{+105.18}_{-3.18}$	$21.44^{+205.05}_{-21.44}$	$5.32^{+125.68}_{-5.32}$	$10.73^{+7.80}_{-10.73}$
G357.7-0.1	$7.57^{+6.66}_{-7.57}$	$0.49^{+30.87}_{-0.49}$	$3.86^{+74.51}_{-3.86}$	$0.87^{+38.32}_{-0.87}$	$7.58^{+7.04}_{-7.58}$

- Average total particle energy is  $8 \times 10^{49}$  erg.
- ~8% of a the  $10^{51}$  erg released by a supernova goes into accelerating particles.

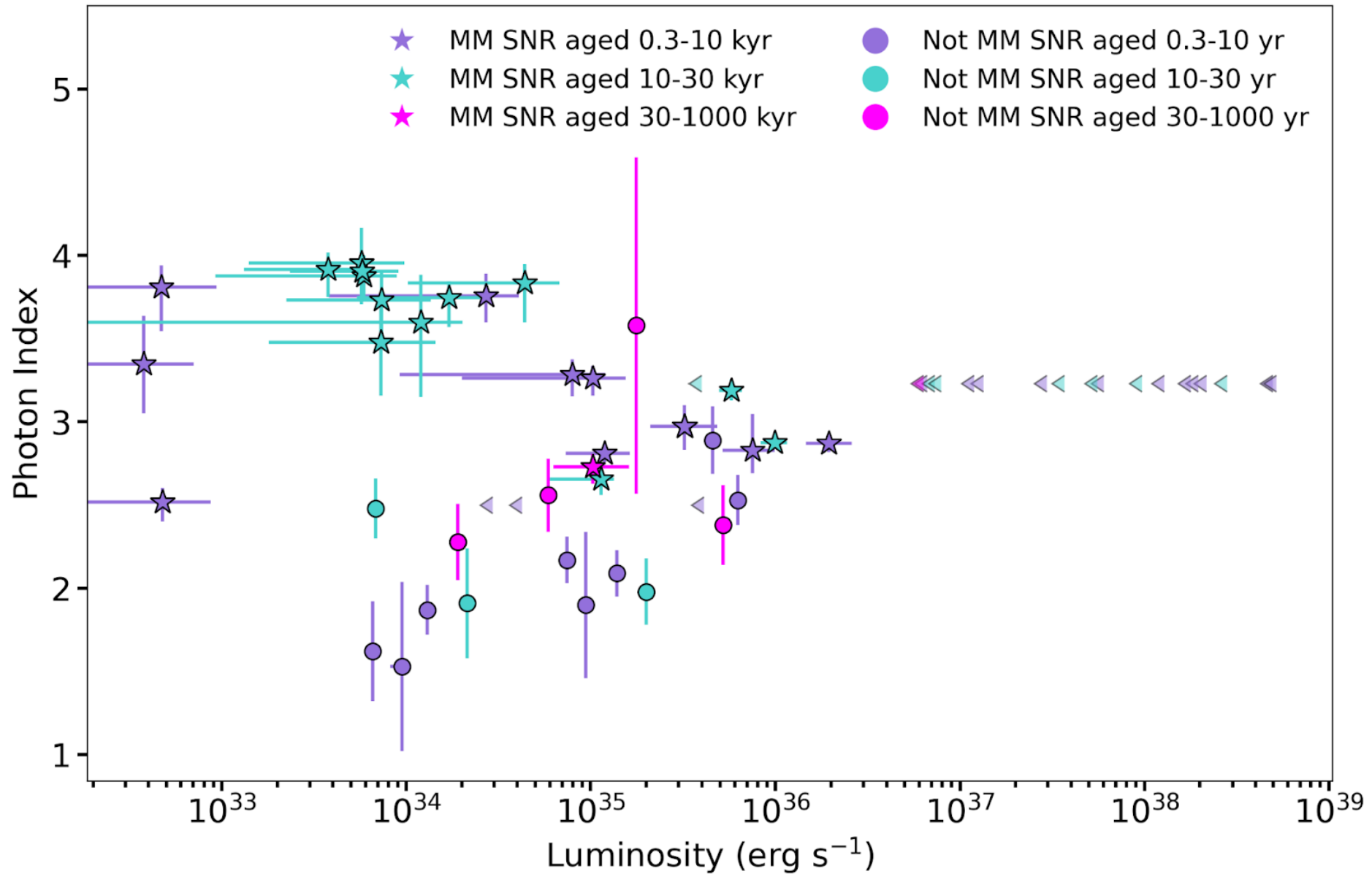
# Summary

- MM SNRs are extremely bright GeV gamma-ray emitters.
- Their dense environment leads to significantly impact the gamma-ray emission from SNRs.
- Potentially only MM SNRs from core-collapse supernovae are detected in gamma-rays.
- MM SNRs have a narrow age range and their average detected age is much higher than non-MM SNRs.
- Neutral pion decay dominates the gamma-ray emission.
- ~8% of a supernova's explosion energy goes into particle acceleration.
- Gamma-ray densities are much higher than those derived using X-rays.

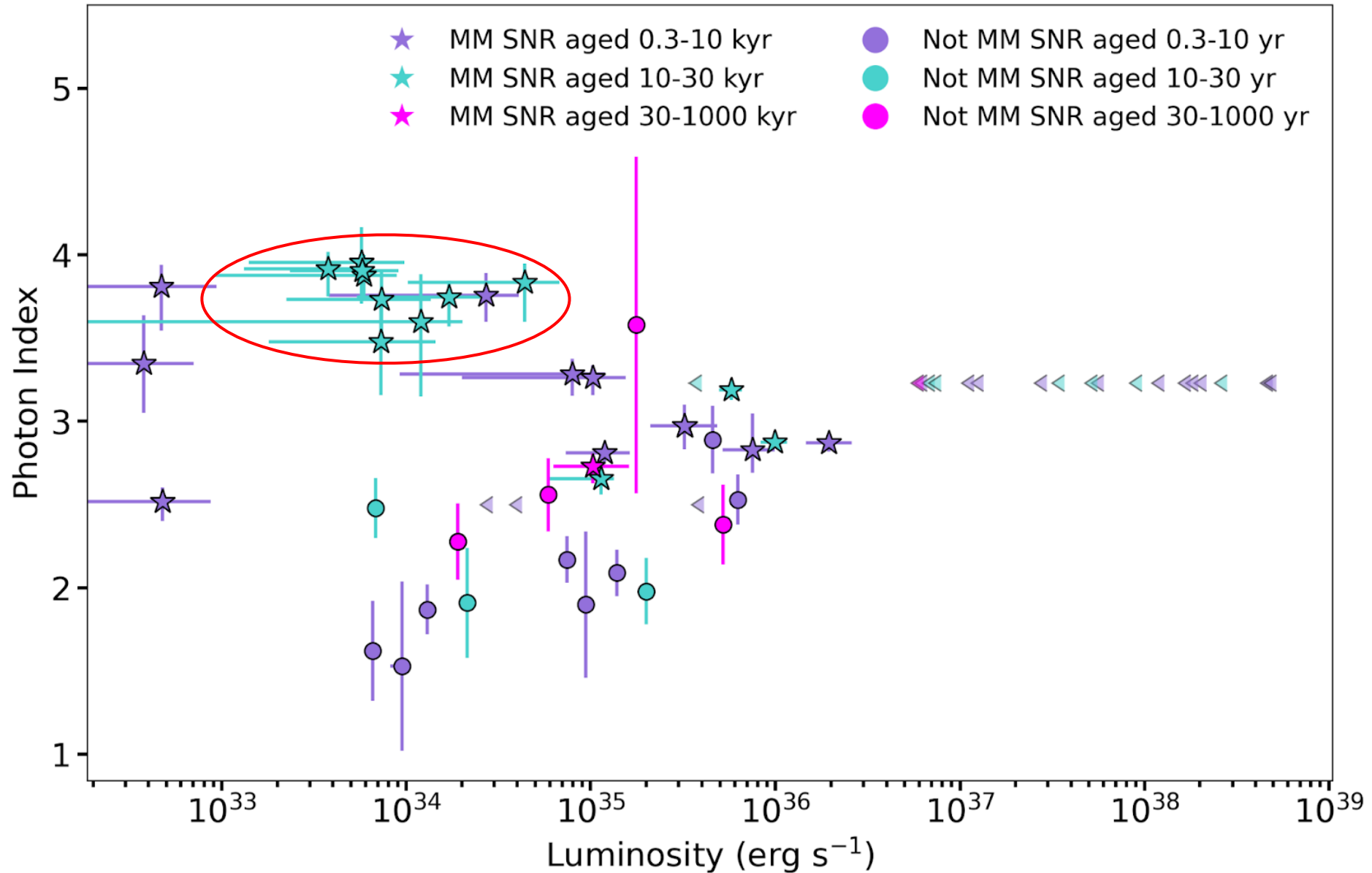
# Future Work with CTA

- CTA will be able to provide a resolution of  $\sim$  few arcmin over an energy range  $\sim 10 - 10^5$  GeV
- Obtain higher resolution data of these MM SNRs compared to Fermi-LAT.
- By using data from both CTA and Fermi-LAT a broader energy range of gamma-ray emission can be analysed.

# Results - Age



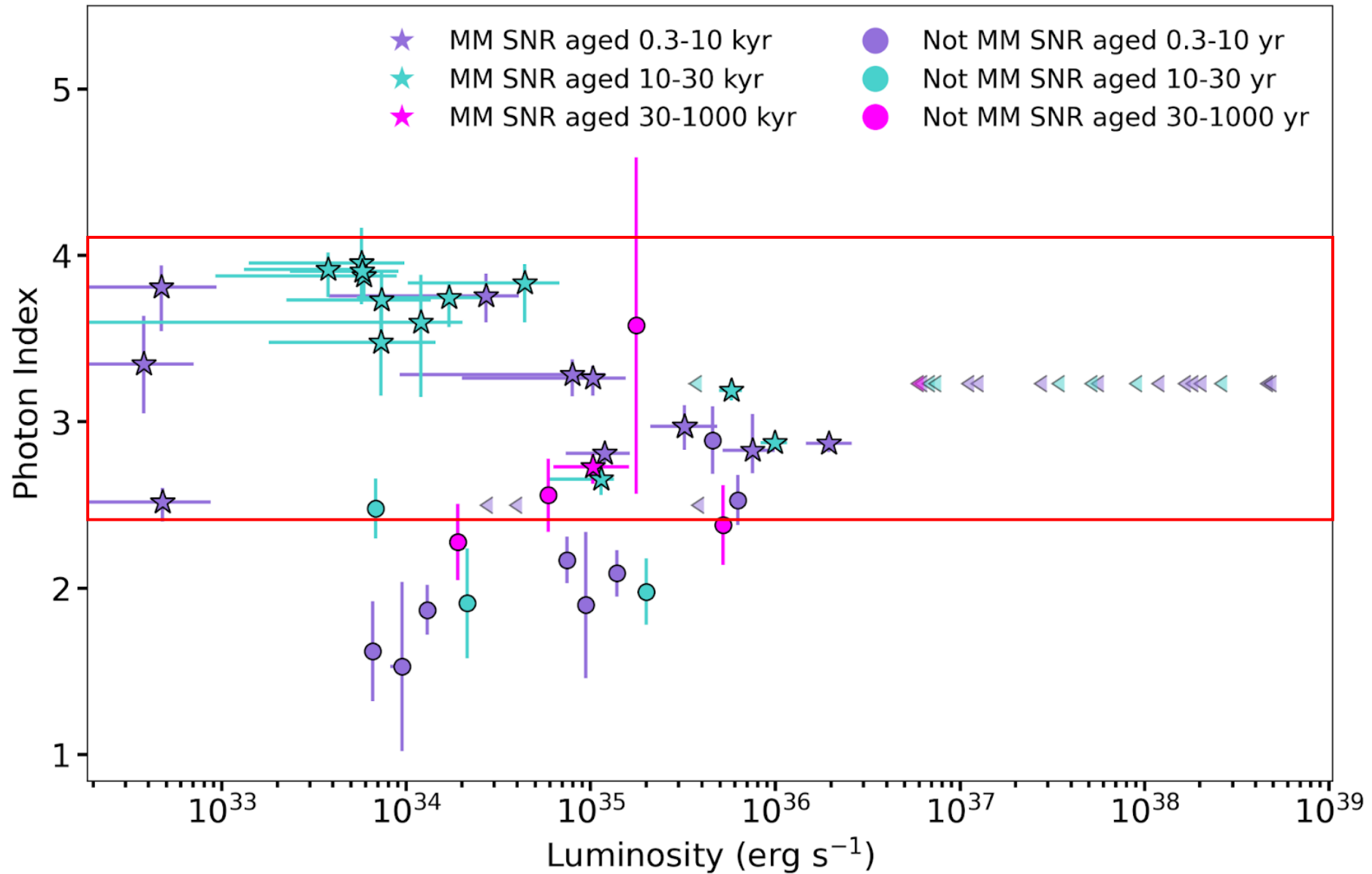
# Results - Age







# Results - Age



# Results - Age

